JOURNAL OF PETROLOGY | VOLUME 47 | NUMBER 8 | PAGES 1591–1610 | 2006 | doi:10.1093/petrology/egl021

Formation of Spinifex Texture in Komatiites: an Experimental Study

FRANÇOIS FAURE[1]*, NICHOLAS ARNDT[2] AND GUY LIBOUREL[1,3]

[1]CENTRE DE RECHERCHE PÉTROGRAPHIQUE ET GÉOCHIMIQUES, CNRS-UPR2300, BP 20, 54501 VANDOEUVRE LES NANCY, FRANCE

[2]LABORATOIRE DE GÉODYNAMIQUE DES CHAÎNES ALPINES, UMR 5025, UNIVERSITÉ JOSEPH FOURIER, BP 53, 38041 ST MARTIN D'HÈRES, FRANCE

[3]ECOLE NATIONALE SUPÉRIEURE DE GÉOLOGIE-INPL, BP 40, 54501 VANDOEUVRE LES NANCY, FRANCE

RECEIVED OCTOBER 14, 2004; ACCEPTED MARCH 24, 2006; ADVANCE ACCESS PUBLICATION APRIL 27, 2006

The formation of platy olivine spinifex, the texture that characterizes komatiite lavas, has long been enigmatic. A major problem is that the dendritic morphology of the olivine resembles that of crystals grown in laboratory experiments at high cooling rates (>50°C/h), but at the position where these textures form, up to several meters below the komatiite flow top, the cooling rate cannot have been greater than 1–5°C/h. We performed experiments that demonstrate that the platy habit of spinifex olivine or pyroxene is a consequence of slow cooling of ultramafic magma in a thermal gradient (7–35°C/cm). The charges were cooled at rates between 2 and 1428°C/h and, even at the low cooling rates, the thermal gradient led to constrained growth and the development of preferentially oriented dendritic crystals with morphologies like those in natural platy spinifex-textured lavas. Under these conditions, olivine starts to crystallize at temperatures well below the equilibrium liquidus temperature (37°C < –ΔT< 56°C) depending on the composition of the starting material. When the cooling rate is high, the thermal gradient has a negligible effect on the texture and the crystals have a random orientation, like that in the upper parts of komatiite flows.

KEY WORDS: *komatiite; spinifex; cooling rate; experimental petrology; thermal gradient*

INTRODUCTION

Spinifex is one of the most spectacular magmatic textures. The most striking examples comprise large olivine plates that form parts of giant, decimeter-sized dendritic crystals that are oriented perpendicular to the roof of the komatiitic unit (Fig. 1). The morphology of these large, preferentially oriented crystals has not previously been reproduced experimentally (Donaldson, 1982; Ginibre *et al.*, 1997).

Spinifex-textured komatiite flows are generally subdivided into three major units, as illustrated in Fig. 1. A thin (1–10 cm) olivine porphyritic upper chilled margin (A_1) is underlain by a ~5–50 cm thick A_2 layer that consists of fine, skeletal and dendritic, randomly oriented olivine crystals embedded in a glassy matrix. Then follows a layer of coarse-grained platy spinifex (A_3) that is dominated by large (up to 1 m long), preferentially oriented, dendritic crystals of olivine. The A_3 layer can be up to several meters thick, and it overlies an olivine cumulate (B_1–B_4) of equal or greater thickness.

A key element in discussions about the origin of spinifex textures is an apparent discrepancy between the cooling rates required to grow skeletal or dendritic olivine crystals in laboratory experiments and those that prevailed during the solidification of komatiitic magmas, either in lava flows or in intrusions. Cooling rates in the thin uppermost layer of a submarine komatiite flow must have been extremely high, as a result of rapid loss of heat from hot komatiite to seawater, but once the crust had reached a thickness of >1 m, the cooling rate in the interior of the flow would have decreased considerably because heat would then be lost primarily by conduction through the crust. Donaldson (1982) estimated that cooling rates in the A_3 layer of a typical 5–10 m thick komatiite flow were <1°C/h. In contrast, to reproduce the dendritic morphology of platy spinifex olivine crystals in normal dynamic cooling laboratory experiments requires cooling rates >50°C/h (Donaldson, 1982).

*Corresponding author. Telephone: +33-383-594226. Fax. +33-383-511798. E-mail: ffaure@crpg.cnrs-nancy.fr

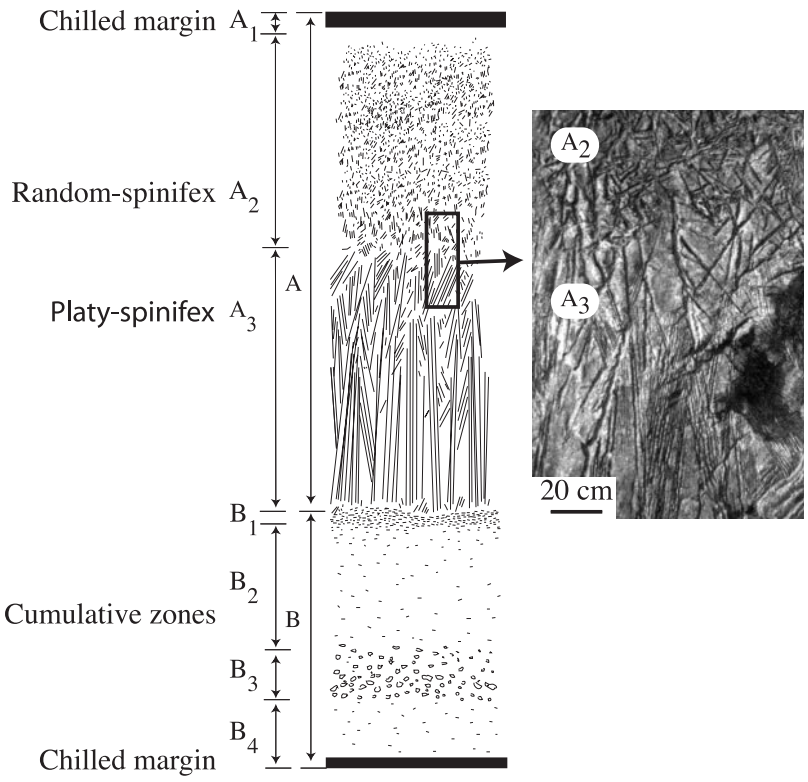

Fig. 1. Sketch of a komatiite flow showing variations in the size and morphology of olivine crystals (from Pyke *et al.*, 1973). The photograph of a komatiite flow from Munro Township, Ontario, shows the contact between the fine, randomly oriented olivines of the A_2 layer and the larger, preferentially oriented, platy olivines of the A_3 layer.

Although numerous solutions to the 'spinifex paradox' have been proposed, none is entirely satisfactory. Donaldson (1982) attributed the differences in morphology between experimentally and naturally crystallized olivine to differences between the MgO contents in the experimental charges and komatiite lavas. When he wrote his paper in 1982 he noted that no experiments had been conducted on samples with MgO contents as high as those of spinifex-textured komatiites, and he suggested that spinifex texture might form only in highly magnesian liquids. More recent experiments have shown, however, that the discrepancy persists even for more magnesian compositions, such as those of chondrules in primitive meteorites (Lofgren, 1989). In addition, preferentially oriented crystals typical of platy spinifex have never been reproduced in laboratory experiments. Turner *et al.* (1986) proposed that spinifex textures could be explained by rapid cooling caused by vigorous internal convection of the komatiite flow. This condition is unlikely to be met, however, in normal komatiite flows (Renner, 1989). Aitken & Echeverria (1984) and Arndt (1994) proposed that spinifex texture results from crystallization of komatiitic magma that had become superheated during rapid ascent from its mantle source. This hypothesis was not supported in experiments by Ginibre *et al.* (1997), who showed that superheating does not enhance the capacity of komatiite liquid to form skeletal crystals at low cooling rates. Shore & Fowler (1999) argued that hydrothermal circulation through the upper crust of a flow, and radiative heat transfer along olivine crystals, could have increased the cooling rate in the platy spinifex zone. These factors probably diminish the discrepancy, but they do not provide a complete solution to the 'spinifex paradox'.

Grove *et al.* (1994, 1996, 2002) and Parman *et al.* (1997) proposed a very different explanation. In their earlier papers they suggested that the komatiites of the Barberton greenstone belt in South Africa, the type area of komatiite, did not erupt as lava flows but crystallized in a sill complex that intruded at a significant depth (~6 km) in the volcanic sequence. In their model, spinifex forms during the crystallization of hydrous, intrusive komatiite. Field studies by Dann (2000, 2001) have shown, however, that these komatiites, like those in most other areas, erupted as lava flows. Further comments on the wet komatiite hypothesis have been given by Arndt *et al.* (1998) and Arndt (2003).

If the formation of spinifex texture cannot be attributed solely to the nature or composition of the komatiite liquid, an explanation for its origin must be sought in

the physical conditions that prevailed during crystallization of the upper part of a komatiite flow. In every crystallizing magmatic unit, a thermal gradient exists within the outer crust that separates the hot liquid interior from the colder surroundings. In a basaltic lava flow, the temperature difference between liquidus and solidus is small (~100°C) and only a very thin layer of partially molten rock separates magma from totally solid crust. In komatiite, the temperature difference between liquidus and solidus is as much as 500°C, resulting in a thick zone in which olivine crystals are bathed in silicate liquid (Arndt, 1976, 1994). In our study we tested the hypothesis that spinifex texture forms by crystallization of magma in the temperature gradient across this zone.

EXPERIMENTAL PROCEDURES

To explore the effect of a thermal gradient on the crystallization behavior of olivine and pyroxene, we conducted a series of experiments on four compositions in the system CaO–MgO–Al_2O_3–SiO_2. The specific compositions, three with olivine as the liquidus phase named Fo III, Fo VI and Fo VII and one with clinopyroxene on the liquidus named Cpx I, were chosen to match the compositions of natural komatiites. Starting materials (Table 1) were mixtures of reagent-grade oxides that had been melted above their liquidus temperatures for 6 h, quenched in water, and then ground to fine powder in an agate mortar. The resulting glass powder was loaded into 6–10 cm long graphite crucibles that were placed in the upper part of a vertical high-temperature, gas-mixing furnace (GERO HTRV 70-250). Graphite, instead of platinum, was used to minimize the wetting of the container wall by the ultramafic melt. Depending on the exact location of the graphite crucible above the hot zone of the furnace, the thermal gradient varied between 34·4 and 2·5°C/cm (Fig. 2). The thermal gradient was determined by measuring temperatures with a $PtRh_6/PtRh_{30}$ thermocouple at the end of a ceramic rod as the thermocouple was moved up from the hot centre to the upper cold end of the furnace. The thermocouple had previously been calibrated against the melting points of gold (1064°C) and palladium (1552°C).

A flow of Ar maintained a reducing atmosphere in the furnace to avoid oxidation of the graphite crucible. At the start of each experiment the tube was held entirely above the liquidus temperature of the starting material. After melting, the length of the experimental charge was reduced from 6–10 cm to about 3–5 cm as a result of compaction and release of air bubbles in the starting material.

To explore the role of the thermal gradient on crystallization, a series of experiments was undertaken in which the cooling rate and the thermal gradient were varied independently. The majority of experiments were carried out with cooling rates between 2 and 5° C/h, rates that correspond to those in the interiors of lava flows but are an order of magnitude lower than those needed to grow dendritic crystals in conventional dynamic crystallization experiments (Donaldson, 1982; Faure *et al.*, 2003*a*). The thermal gradient was varied from 18·4 to 20·2°C/cm, also like those calculated for the upper zones of komatiite flows. To explore the effects of more rapid cooling, as in the outer chill zones of lava flows, we also conducted experiments at cooling rates of 10 and 1428°C/h. Two additional series of experiments were also performed: in the first, the charges were cooled slowly, at 5°C/h, to crystallize spinifex texture and then held isothermally for several hours; in the second, the cooling rate was the same (5°C/h) but the thermal gradient was much lower (2·5–3·2°C/cm).

Another experimental procedure was used to explore the influence of crystals present in the charge before crystallization in the thermal gradient. After a period of melting above the liquidus temperature, the charge was cooled rapidly until the temperature at the top of the charge was just below the liquidus whereas the temperature at the base of the charge remained above the liquidus. The charge was maintained in this thermal configuration for 1 h and then was slowly cooled at 5°C/h in a large thermal gradient.

Each experiment was terminated by dropping the charge into water, generally before the crystallization front had reached the end of the capsule. The charge was then cut along its long axis and polished, and the positions of olivine and pyroxene crystallization fronts were measured. The charges were studied in thin section and by scanning electron microscopy (SEM), and glass compositions were analyzed on the Cameca SX50 electron microprobe at the Université Henri Poincaré, Nancy.

Table 1: Bulk compositions of starting material determined by electron microprobe

	Fo III	Fo VI	Fo VII	Cpx I
SiO_2	50·71	51·35	46·72	53·80
Al_2O_3	13·55	14·54	13·06	11·60
MgO	17·80	16·36	22·34	14·44
CaO	17·93	17·73	17·86	19·43
Liquidus phase	olivine	olivine	olivine	clinopyroxene
T liquidus (°C)	1342	1320	1429	1305
Second phase	clinopyroxene	clinopyroxene	n.d.	anorthite
and T (°C)	1284	1280		1267

n.d., not determined.

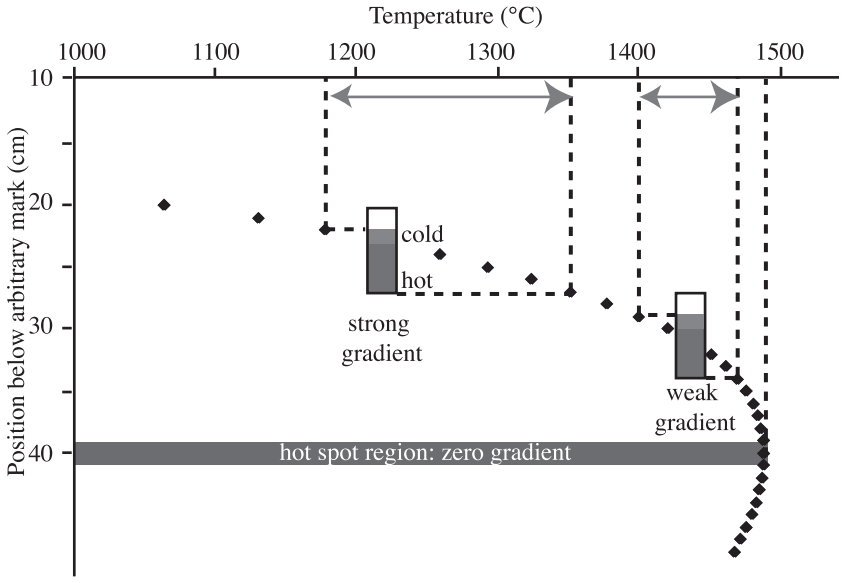

Fig. 2. Sketch of the experimental configuration showing that the thermal gradient varies from weak (7°C/cm) to strong (35°C/cm), depending on the vertical position of the capsule within the furnace, shown as a rectangle with grey layers representing the experimental charge. Conventional dynamic crystallization experiments are conducted with the charge at the center of the furnace where the thermal gradient is minimal.

Figure 3 shows a scanned image of a typical experimental charge (Fo VI-18), which was cut along its length and transformed into a thin section. In this type of image, the olivine crystals are nearly transparent and very difficult to distinguish from the glass, and only the clinopyroxene crystals are visible. However, olivine crystals are readily identified with SEM or optical microscope and by using these methods we were able to establish accurately the crystallization fronts of both olivine and pyroxene. Because our calibration provided an accurate relationship between position in the charge and temperature, the temperature at the onset of olivine and clinopyroxene crystallization could be determined with precision. This feature, a major advantage of the experimental set-up, gave us information about the crystallization history of rapidly cooled silicate liquids that is totally inaccessible in normal dynamic crystallization experiments.

EXPERIMENTS WITH OLIVINE AT THE LIQUIDUS

Olivine in komatiite flows displays a wide variety of habits, from equant solid polyhedral crystals in the chilled margins and cumulate zones, to fine, randomly oriented skeletal grains in the uppermost part of the spinifex zone, and to large, complex dendritic crystals deeper in the flow (Fig. 1). In our experiments, we were able to reproduce all these textures. We found that the morphology of olivine crystals depends critically on the experimental conditions, as illustrated in Table 2.

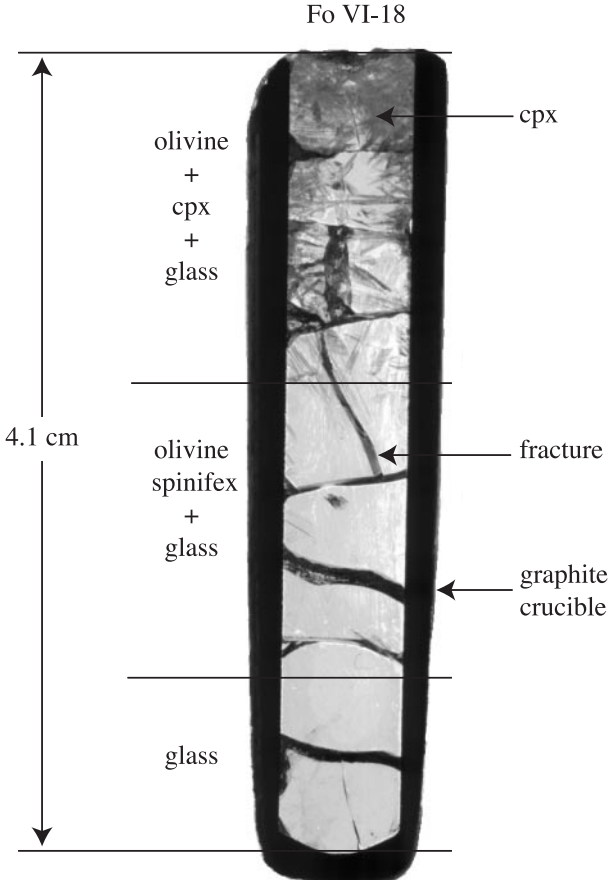

Fig. 3. Scanned image of an experimental charge cut along its length and polished.

Table 2: Experimental conditions and results of experiments performed with compositions that have olivine at the liquidus

Run	Cooling rate(°C/h)	Thermal gradient(°C/cm)	Starting temperature(°C)	Charge length(cm)	Total run duration(h)	Olivine-in(°C)	Degree of undercooling(°C)	Clinopyroxene-in(°C)
FoVI-11	5	2·5	1327	6·3	2·2	>1317		
FoVI-13	5	3·2	1325	4·2	1	1320		
FoVI-14	5	20·2	1358	4·5	20	1261	62	
FoVI-15	5	20·7	1375	4·1	39	>1254		1236
FoVI-17	5	19·9	1363	4·4	30	1265	54	1231
FoVI-18	5	19·4	1373	4·1	34	1269	50	1238
FoVI-20	5	19·4	1366	4·4	25	1262	57	
FoVI-21	5	18·4	1395	4·3	30	1262	57	
FoVI-23	10	20	1374	4·4	17	1260	59	1232
FoVI-22	5	18·9	1356	4·1	25 + 4†	1282	37	
FoVI-24	5	30·6	1373	4·3	25 + 9†	1307	12	
FoIII-1	5	19·4	1371	5·2	28	1293	49	1238
FoIII-2	5	20	1371	3·5	42	>1249		1220
FoIII-3	5	20·3	1371	4·6	50	>1208		>1208
FoIII-6	1428	20	1371	4·9	0·16	>1247		1224
FoIII-11	2	19·5	1371	4·8	79	1287	55	1226
FoIII-24	5	7·3	1344	5·3	18·2	1290	52	
FoVII-6	5	25·8	1404	5·5	46·5	>1295		
FoVII-7	5	25·2	1422	5·3	37·5	>1347		
FoVII-8	5	21	1422	4·6	23·5	1392	36	
FoVII-11	5	18·6	1483	4·2	23·5	1394	34	
FoVII-12	5	19·9	1473	4·2	27·8	1391	37	

*At the top of the charge.
†Isothermal step of 4 and 9 h after the slow cooling of 25 h.

Slow cooling rate and large thermal gradient

Texture

Up to three phases were observed in the experimental charges—olivine, clinopyroxene, and glass that represents quenched silicate liquid (Fig. 4a). In experiments undertaken at typical cooling rates (2–5°C/h) and in normal thermal gradients (~20°C/cm), sparse, long and thin blades of olivine extend a centimeter or more below a front of more densely crystallized pyroxene-rich material. These textures are similar to what is seen in natural komatiites (Fig. 4b). At the olivine crystallization front, near-vertical olivine crystals range in habit from thin (Fig. 4a) to broad (Fig. 5a and b), depending on the orientation of the section. When the olivine grains are observed with a petrographic microscope in sections parallel to the (010) plane, these large olivine grains are seen to form parts of dendritic crystals (Fig. 6) whose overall habit is similar to that of swallowtail olivine fibres produced in dynamic cooling experiments (Faure *et al.*, 2003*a*).

The large dendritic olivine plates are oriented perpendicular to the cooling front (Figs 4a and 5a). When a crystal is oriented slightly obliquely to this direction, the crystal growth stops then restarts with an orientation closer to parallel to the thermal gradient (Fig. 7). The growth of more oblique crystals terminates when the crystal reaches vertically oriented grains. This process, which is the probable cause of the preferred orientation of spinifex-textured crystals in komatiite lava flows, is particularly well observed in charges where there are few spinifex crystals.

In cross-section, olivine forms parallel rods with planar or lumpy outlines (Figs 4a and 5a, b). In some samples, the rods seem to have formed by juxtaposition of skeletal-shaped units (Fig. 5a and b) in a similar way to the growth of dendritic olivine in conventional dynamic crystallization experiments, as observed at nanometer scale using transmission electron microscopy (Faure *et al.*, 2003*b*).

The matrix of the charges consists of pyroxene and glass. Pyroxene crystals are randomly distributed in the glass, suggesting an absence of a systematic relation between the crystallographic orientation of pyroxene

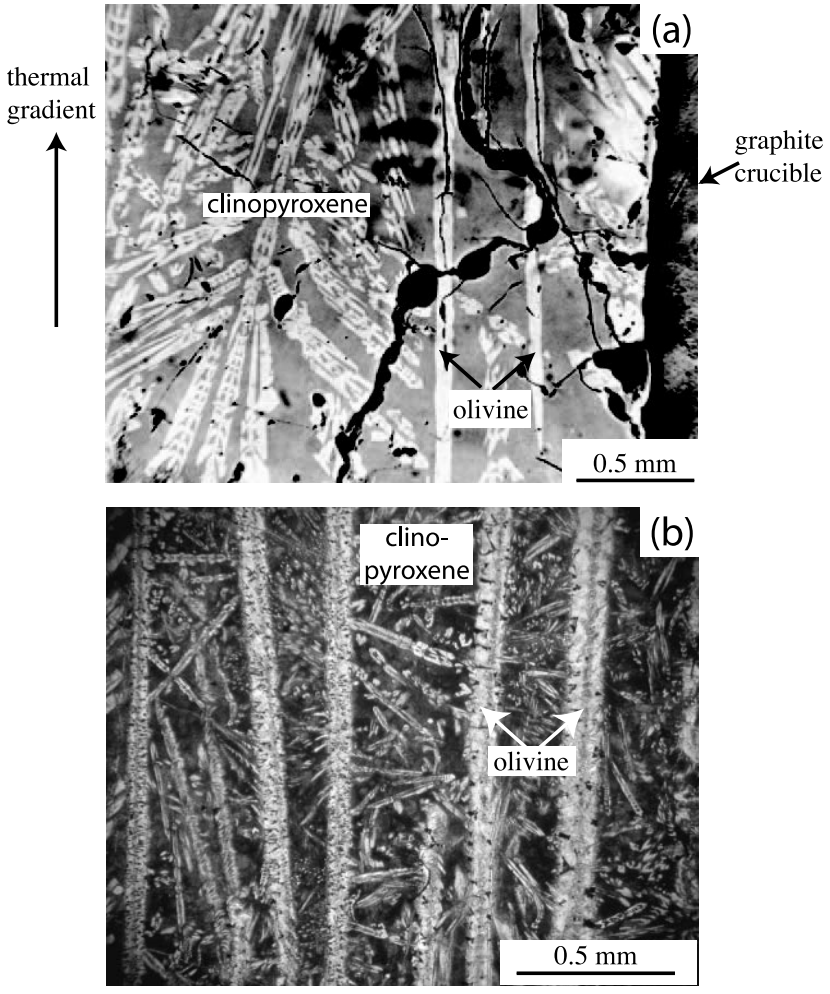

Fig. 4. Photomicrographs comparing olivine and pyroxene grains in (a) an experimental charge (Fo III-2) and (b) natural spinifex-textured komatiite (Alexo flow, Abitibi greenstone belt). It should be noted that the distinctive morphology and the preferential orientation of olivine crystals in natural spinifex-textured komatiite are reproduced in the experiments. Typical pyroxene textures are also developed, with pyroxenes crystallizing between the olivine plates just as in the natural lava.

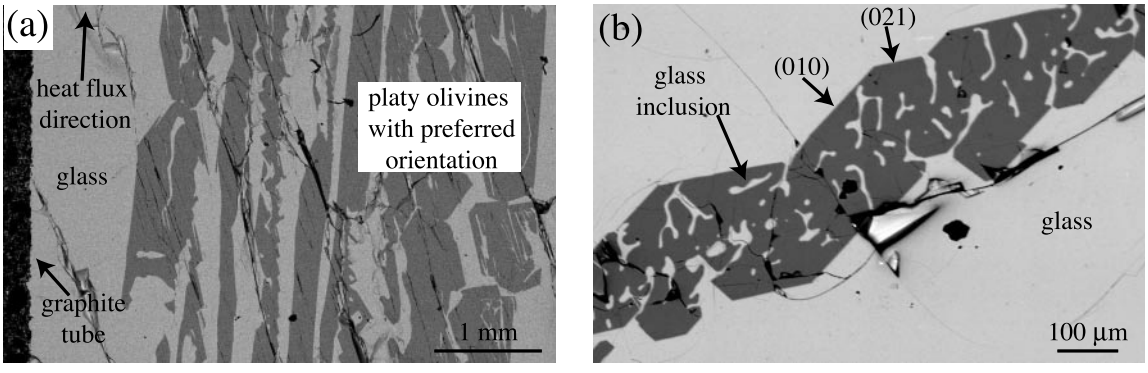

Fig. 5. Backscattered electron images showing platy spinifex olivine crystals. (a) Platy spinifex crystals are elongated in the heat flux direction, which is parallel to the capsule wall (Fo VII-6: cooling rate 5°C/h, thermal gradient 25·8°C/cm). (b) Large olivine blade cut at an oblique angle to the (100) plane. The blade seems to have formed by the juxtaposition of units that have a pseudo-hexagonal shape limited by (010) and (021) faces (Fo III-11: cooling rate 2°C/h, thermal gradient 19·5°C/cm).

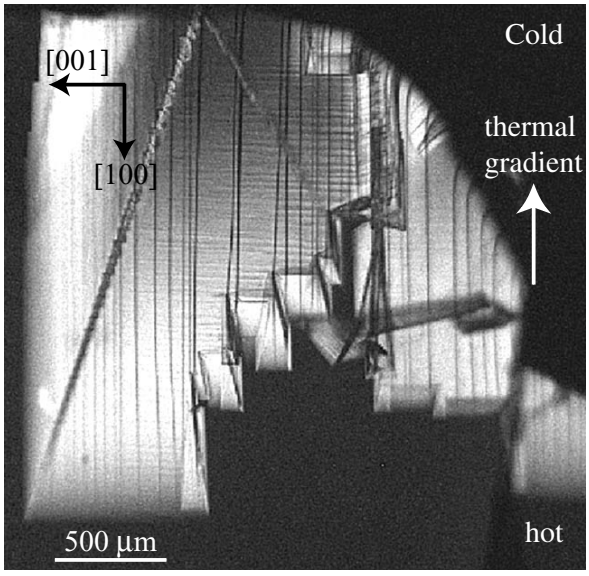

Fig. 6. Transmitted-light photomicrograph showing a spinifex olivine crystal observed in section parallel to (010) plane. (Fo VI-18: cooling rate 5°C/h, thermal gradient 19·4°C/cm).

Fig. 7. Transmitted-light photomicrograph showing a contact between two olivine crystals. The first crystal (above) has grown slightly obliquely to the heat flux direction. Its growth has stopped and a new crystal (below) has developed on the first one but with a direction of elongation parallel to the thermal gradient (Fo III-11: cooling rate 2°C/h, thermal gradient 19·5°C/cm).

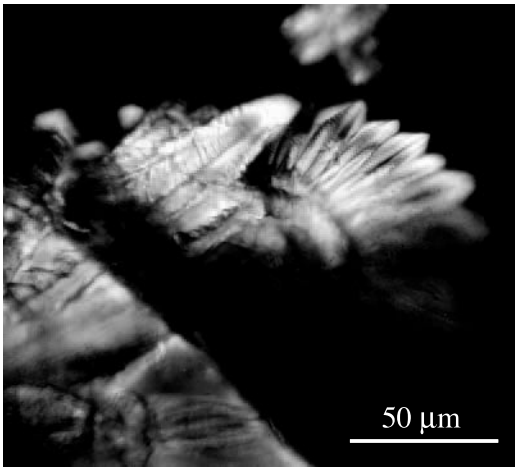

Fig. 8. Transmitted-light photomicrograph (crossed polars) displaying plumose clinopyroxene crystals with prominent radiating fibers (Fo III-2: cooling rate 5°C/h, thermal gradient 20°C/cm).

Table 3: Electron microprobe analyses of clinopyroxenes

	Equilibrium pyroxene	Microspinifex pyroxene Fo-VI-15	Microspinifex pyroxene CPX-I-1	Macrospinifex pyroxene CPX-I-1
SiO_2	55·11	51·98	53·92	54·24
Al_2O_3	1·81	6·41	4·20	2·79
MgO	20·05	18·42	19·61	19·86
CaO	23·01	23·17	22·25	23·09

See Table 2 for run conditions.

and olivine crystals. The clinopyroxene crystals between the larger, vertically oriented olivine grains have plumose and chain morphologies (Fig. 4a) with shapes very similar to those observed in natural komatiites (compare Fig. 4a and b). In particular, the strongly curved shape of plumose pyroxene is reproduced (Fig. 8). This peculiar crystal morphology, which resembles that of spherulites, is observed throughout the zone in which the clinopyroxene crystallizes, but most conspicuously directly at the pyroxene crystallization front. The plumose clinopyroxene crystals have the Al-rich compositions (Table 3) characteristic of pyroxene in natural komatiite flows (Nesbitt, 1971; Arndt & Fleet, 1979). By comparison, clinopyroxene grown in equilibrium conditions, as in previous experiments undertaken to determine the liquidus phase relations given in Table 1, has low Al contents, as shown in Table 3.

Position of olivine and clinopyroxene crystallization fronts

As noted in the section on experimental procedure, the positions of the olivine and clinopyroxene crystallization

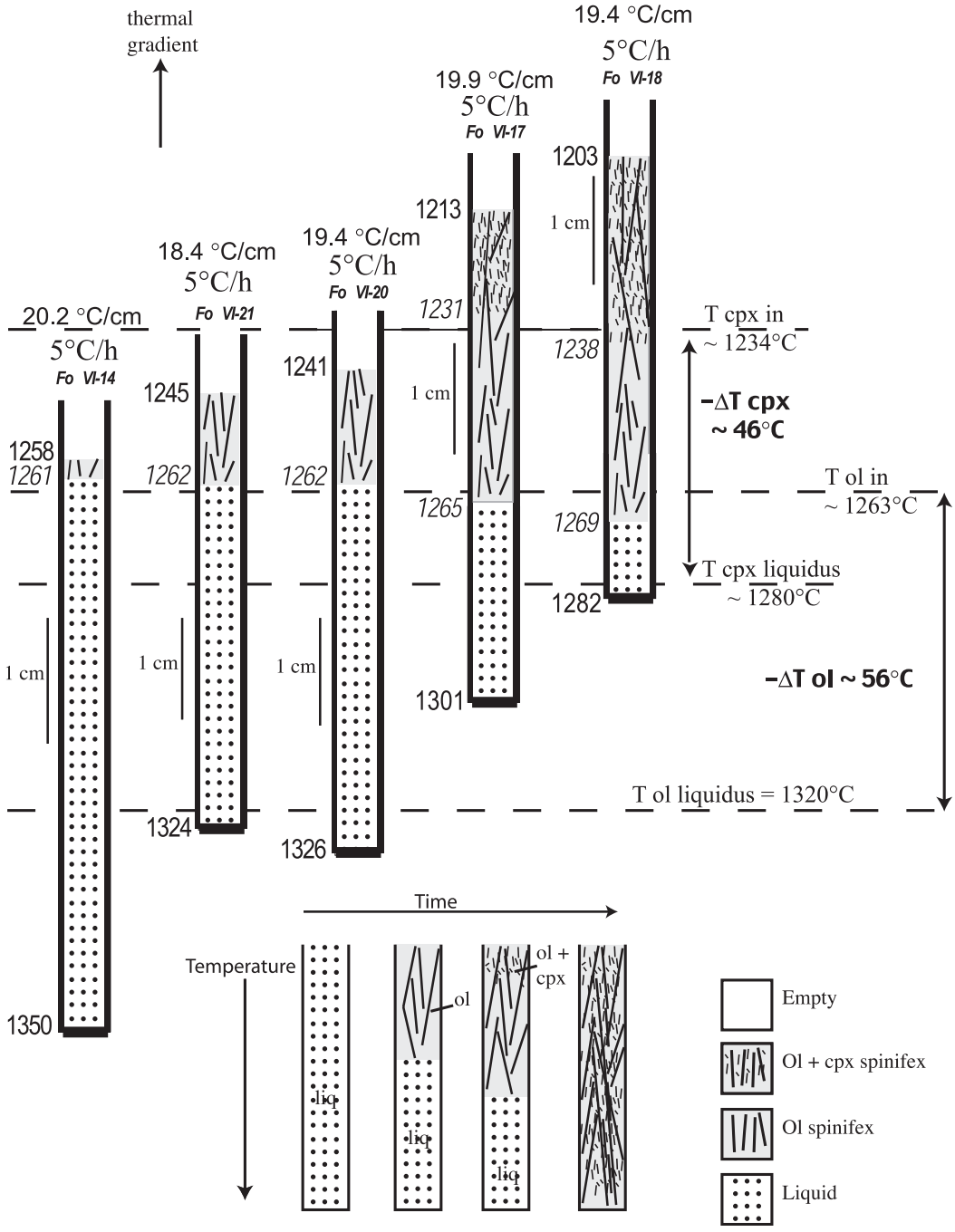

Fig. 9. Sketches summarizing the results of experiments performed with Fo VI starting composition. Each diagram shows the positions of olivine and pyroxene crystallization fronts at the time of quenching. The four lower diagrams summarize the mode of crystallization of spinifex in the upper part of a komatiite flow. Calibration of the relation between temperature and position in the furnace allowed us to determine the temperature of onset of olivine and pyroxene crystallization (labeled 'T ol in' and 'T cpx in'). These temperatures are well below the equilibrium liquidus temperatures ('T ol liquidus' and 'T cpx liquidus') and define the degree of undercooling ($-\Delta T$).

fronts allow us to estimate the temperatures at the onset of olivine and clinopyroxene crystallization. Seventeen experiments were performed to determine accurately the position of these crystallization fronts as a function of cooling rate, thermal gradient and liquid composition (Table 2). From equilibrium experiments (Table 1) we know that in the Fo VI composition, the liquidus temperatures of olivine and clinopyroxene are 1320°C and 1280°C, respectively. From Fig. 9 we see that in our thermal-gradient experiments, the base of the olivine

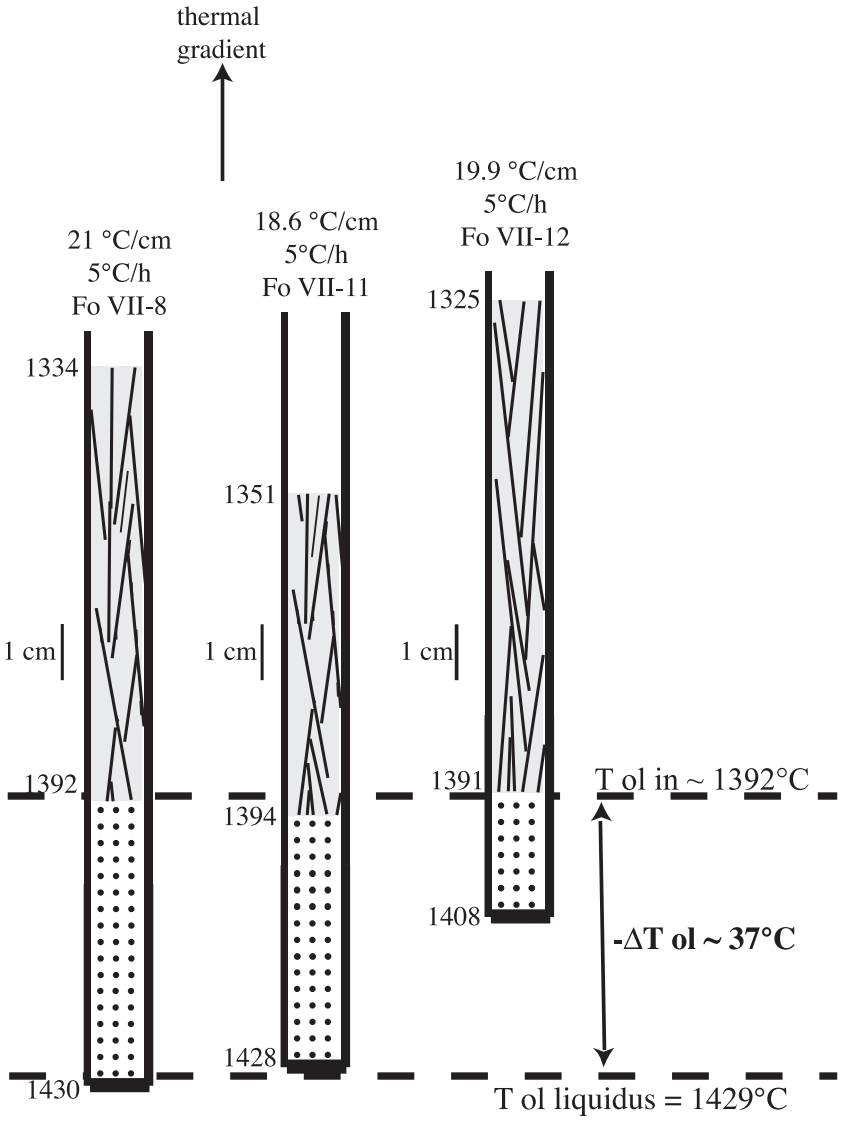

Fig. 10. Sketches displaying the positions of the olivine crystallization front at the time of quenching in experiments performed with Fo VII starting composition. All charges were quenched before crystallization of clinopyroxene.

crystallization front lies about 3 cm above the 1320°C isotherm. For the thermal gradient in the furnace, this corresponds to a large temperature difference between the equilibrium liquidus and the onset of olivine crystallization, or a degree of undercooling ($-\Delta T$) of about 56°C. The pyroxene crystallization front has a $-\Delta T$ of about 46°C.

Starting composition Fo VII shows similar phase assemblages but different degrees of undercooling (Table 2 and Fig. 10). This composition is richer in MgO than Fo VI and displays a smaller $-\Delta T$ for olivine of about 37°C. Similarly, Fo III (Fig. 11), which has a MgO content only slightly higher than Fo VI, has a slightly lower $-\Delta T$ value for olivine (52°C) and a higher value for pyroxene (56°C).

Absence of the Soret effect

When a temperature gradient is present, chemical diffusion can produce compositional zonation in an initially homogeneous liquid, a phenomenon known as the Soret effect [see Latypov (2003) for a recent review]. To test whether this happened in our experiments, we analyzed glass compositions at 1 mm intervals along a section from the cold top to the hot base of an experimental charge (Fo III-11). Figure 12 shows that except in the cold upper part of the charge where olivine and pyroxene has crystallized, the glass has a uniform composition, showing that the Soret effect was absent. The compositionally homogeneous zone begins well above the olivine and pyroxene crystallization fronts. This uniformity of chemical composition indicates that dendritic crystallization of sparse,

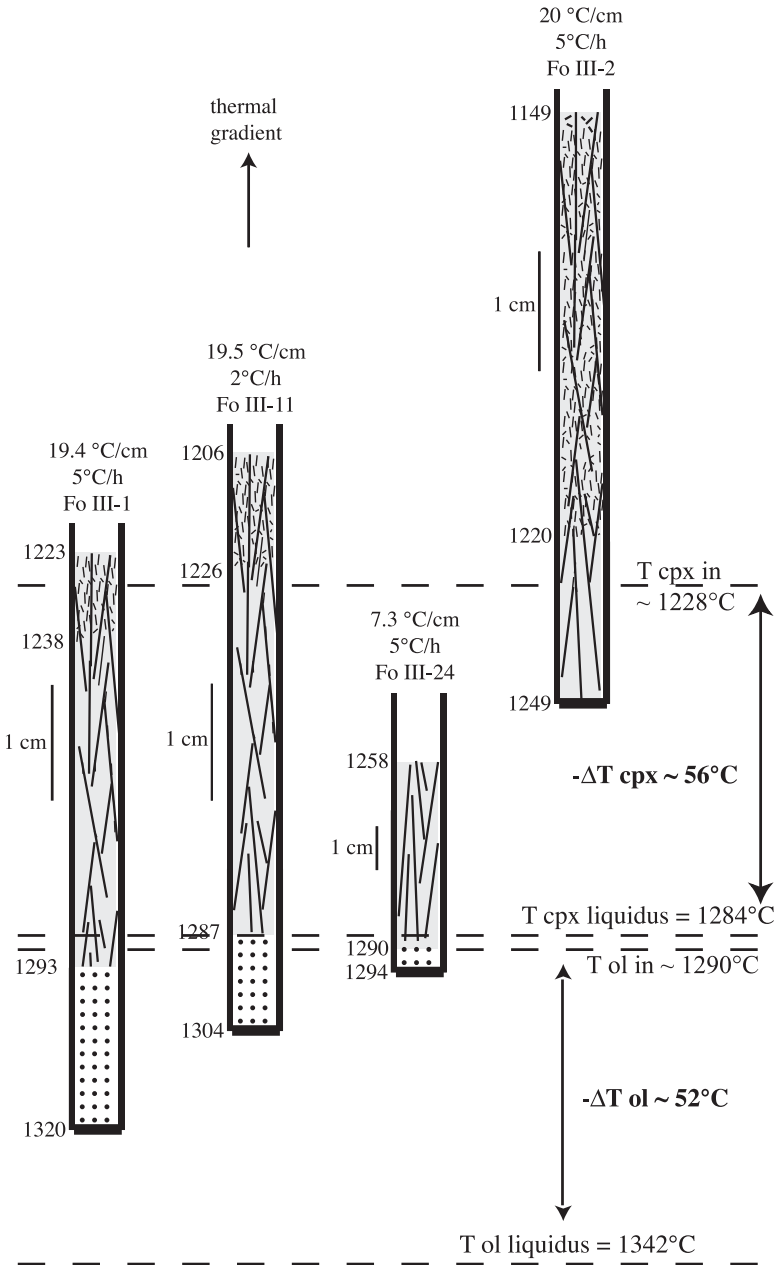

Fig. 11. Sketches displaying the positions of crystallization fronts at the time of quenching in experiments performed with Fo III starting composition.

widely separated olivine crystals changes the liquid composition in only a small region directly adjacent to the crystals (see above) and the small number of olivine crystals does not produce important variation of bulk liquid composition.

Chemical gradient around olivine crystals

In experimental charges containing widely spaced olivine crystals, microprobe analysis of glass immediately adjacent to a crystal reveals a narrow zone (<100 μm) of olivine-depleted (MgO-poor, Al_2O_3-rich) liquid (Fig. 13). The shape of this zone—a bulbous front at the tip of the crystal and gradually increasing thickness up the stem—indicates that olivine-poor liquid builds up ahead of the growing crystal. Similar results obtained in boundary layers around dendritic crystals in conventional dynamic crystallization experiments (Faure, 2001; Faure & Schiano, 2005) or observed in rocks (e.g. Roeder *et al.*, 2001, 2003) are

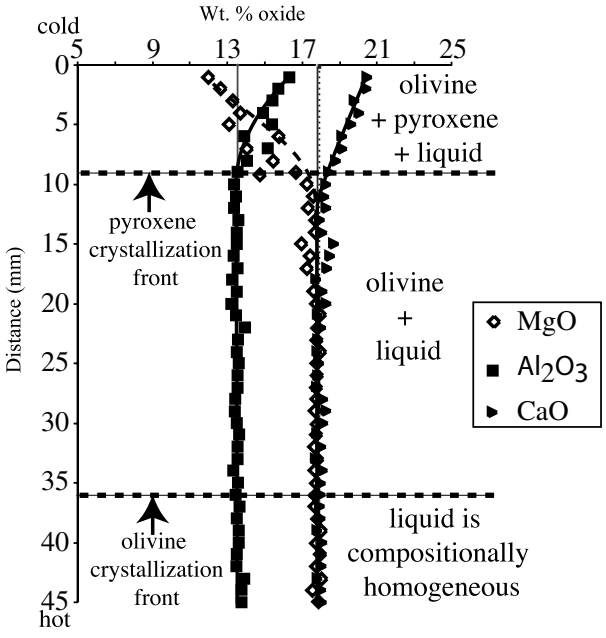

Fig. 12. Weight % of oxides vs position, from the cold top to the hot bottom of the experimental charge, showing absence of the Soret effect in the glass (Fo III-11: cooling rate 2°C/h, thermal gradient 19·5°C/cm).

interpreted in terms of diffusion-controlled crystal growth.

Cooling rate effect

To investigate the effect of more rapid cooling rates, we undertook experiments at 10 and 1428°C/h. In the 10°C/h experiment, olivine crystals no longer have the elongate shapes that characterize the spinifex olivines but instead display hopper morphologies (Fig. 14a). These crystals have more equant skeletal forms, sometimes with the 'baby swallowtail' shape that represents the onset of dendritic growth (Faure *et al.*, 2003*a*). In the charge cooled at 1428°C/h, the olivine crystals have a complex dendritic morphology but they are randomly distributed in the charge (Fig. 14b and Fig. 14c). The morphologies of these crystals are very similar to those produced at similar cooling rates in conventional dynamic crystallization experiments. It is important to note that the temperature of clinopyroxene crystallization remains unchanged in these rapid-cooling experiments, suggesting that the crystallization of a second phase (clinopyroxene in this case) is not affected by the thermal gradient.

It therefore appears that the thermal gradient has little effect on the crystal habit when the cooling rate is high. Under such conditions, the form of the crystals closely resembles that observed in random spinifex-textured lava in the upper A_2 horizon of komatiite lava flows. In contrast, when the cooling rate is stopped after a period of slow cooling (5°C/h), spinifex growth stops as well, and new generation of olivine appears. These new crystals show a hopper shape.

Thermal gradient effect

Two experiments with the Fo VI composition were carried out with a small thermal gradient (2·5 and 3·2°C/cm) and a low cooling rate (5°C/h). In both experiments, clusters or individual crystals of olivine (Fig. 15) had an equant habit rather than the elongate dendritic form of the crystals that grew in larger thermal gradients or at higher cooling rates. Olivine crystals with similar habits are common in chill and B_2 zones of komatiite lava flows (Jerram *et al.*, 2003). The aggregation of crystals into clusters probably resulted from the synneusis process, as proposed by Schwindinger & Anderson (1989) for glomeroporphyritic olivines in Kilauea Iki basalts.

Olivine with an equant habit crystallized only in experiments with very small thermal gradients (<5°C/cm): as the thermal gradient was increased to rates >5°C/cm, the crystals developed a preferred orientation and a dendritic morphology. For example, the form of olivine and pyroxene crystals that grew in the experiment with a moderate thermal gradient of 7·3°C/cm (Fo III composition, experiment FoIII-24 Table 2) is very similar to those of crystals from experiments with greater thermal gradients. [Direct comparison with experiments conducted at low gradients (2·5 and 3·2°C/cm) was not possible because the 7·3°C/cm experiment was carried out using the Fo III composition.] However, because the Fo VI and Fo III compositions are not very different (Table 1), these results suggest that even a weak thermal gradient allows spinifex-like crystals to form, and that only very small thermal gradients prevent this from happening.

EXPERIMENTS WITH PYROXENE AT THE LIQUIDUS

In many spinifex-textured komatiitic basalts, pyroxene, not olivine, is the liquidus mineral. In some rocks, long thin needles with pigeonite cores and augite mantles are oriented perpendicular to the flow top; in others smaller augite crystals with diverse textures and morphologies are the dominant component (Nesbitt, 1971; Fleet & McRae, 1975; Arndt & Fleet, 1979). To investigate the effect of a thermal gradient on the crystallization of pyroxene, we performed four experiments (Table 4) with a starting composition that had pyroxene as the liquidus phase (Table 1).

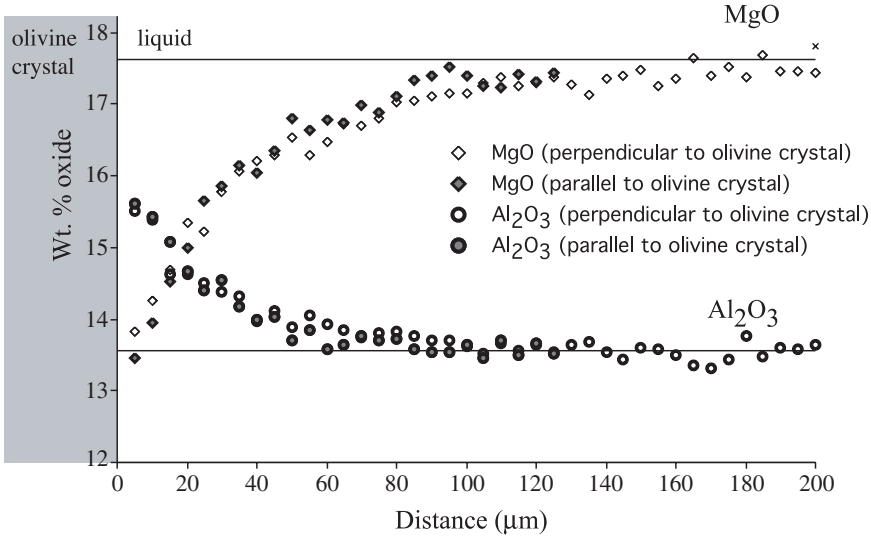

Fig. 13. Compositional profiles at the interface between an olivine crystal and silicate liquid (Fo III-11). Compositions have been measured in the glass along profiles perpendicular and parallel to the direction of propagation of the crystal. The presence of a similar boundary layer at the tip of the crystal and on its side should be noted (Fo III-11: cooling rate 2°C/h, thermal gradient 19·5°C/cm).

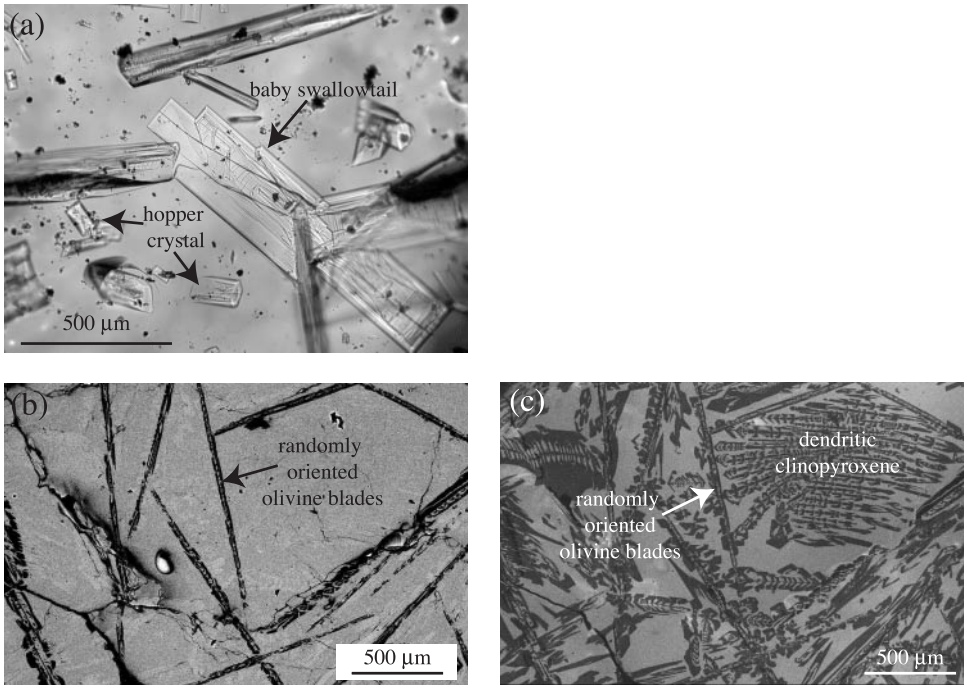

Fig. 14. Morphology and orientation of crystals in rapidly cooled charges. (a) Transmitted-light photomicrograph showing both skeletal hopper olivine crystals and crystals displaying the 'baby swallowtails' that signify the beginning of dendritic morphology. These crystals are set without preferential orientation in glass (Fo VI-23: cooling rate 10°C/h, thermal gradient 20°C/cm). (b) Backscattered electron image showing dendritic olivines randomly distributed throughout the charge (Fo III-6: cooling rate 1428°C/h, thermal gradient 20°C/cm). (c) SEM image of the same zone as shown in (b) but observed in cathodoluminescence mode. Under these conditions, clinopyroxene as well as olivine is visible as black crystals in the gray glassy matrix.

In one experiment (Cpx I-9 Table 4), the entire charge was initially heated above the liquidus. After quenching of this experiment, the charge was totally vitreous, even though the temperature at the top of the charge (1218°C) at the time of quenching had been well below the equilibrium pyroxene liquidus (1305°C, so $-\Delta T = 87$°C; Fig. 16). This result is coherent with classical dynamic crystallization experiments that show that pyroxene

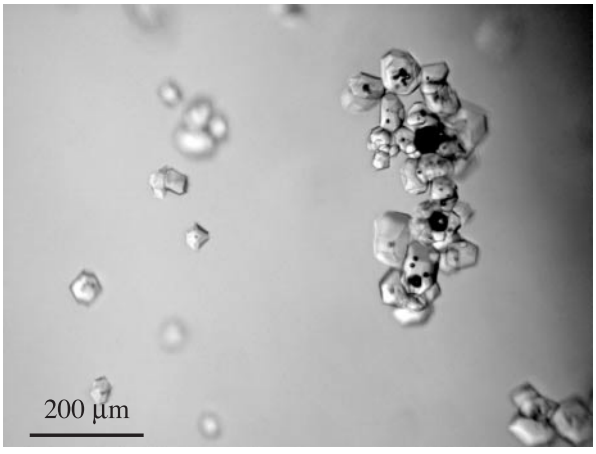

Fig. 15. Transmitted-light photomicrograph of equant olivine crystals in a glassy matrix. The presence of olivine clusters and individual crystals should be noted (Fo VI-13: cooling rate 5°C/h, thermal gradient 3·2°C/cm).

nucleates only at high degrees of supercooling (Kirkpatrick *et al.*, 1976, 1981). The three other experiments were carried out with initial temperatures at the top of the charge that were 18°C to 94°C below the pyroxene liquidus. The textures produced in these experiments are illustrated in Figs 17 and 18. Pyroxene has two distinct habits. The dominant type consists of large elongate crystals that display a strong preferred orientation parallel or sub-parallel to the thermal gradient (Fig. 17b). Each crystal seems to be composed of several tubular units, each with a hollow core. They precisely mimic the morphology of pyroxene in the 'string-beef' spinifex that is present in the upper parts of differentiated komatiitic basalt flows (Arndt *et al.*, 1977; Arndt & Fleet, 1979). As in the natural lavas, the pyroxene crystals are generally more elongate than most olivine spinifex crystals: in some parts of the experimental charges, pyroxene needles ~100 μm thick may exceed 3 cm in length. It is difficult to determine precisely their lengths because of cross-section effects that are always present when crystals have a tubular shape, but the crystals in the charges CPX I-1 and CPX I-10 seem to be stopped only by the graphite at the base of the crucible.

Other pyroxene crystals are smaller, more equant and have random orientations (Fig. 17a). They are observed only in zones where large elongate pyroxene grains have not crystallized and invaded all available space. They have complex morphologies, consisting of various acicular, chain-like or plumose elements, and, as such, they strongly resemble pyroxene grains interstitial to larger oriented needles in natural komatiites. The chemical compositions of the two types of pyroxene in the experimental charges are different. The large, elongate, oriented needles have lower aluminum contents than chain and plumose pyroxenes (Table 3). However, both are richer in aluminum than pyroxene grown in equilibrium conditions.

The second phase in the experimental charge is anorthite, which forms elongate blades between elongate pyroxene needles (Fig. 18a and b). The anorthite blades are oriented at a high angle to the larger pyroxene needles and appear to have nucleated on the pyroxene. The arrangement suggests a crystallographic relationship between anorthite and pyroxene similar to that observed in experiments (Grove, 1978; Lesher *et al.*, 1999) and in spherulites in mid-ocean ridge pillow basalts (Kirkpatrick, 1978; Faure & Schiano, 2004). In all parts of the charges that were quenched from above the solidus temperature, glass remains as an interstitial phase (Fig. 18b); the proportion of glass is far smaller, however, than in the more magnesian charges that crystallized to olivine spinifex textures.

The positions of clinopyroxene and anorthite crystallization fronts are represented in Fig. 16. The onset of the clinopyroxene crystallization is well below the liquidus temperature with a degree of undercooling ($-\Delta T = 37$°C) similar to that in experiments on charges with olivine at liquidus. The anorthite crystallization front displays a very large degree of undercooling ($-\Delta T > 100$°C).

DISCUSSION

Origin of spinifex texture

One of the main results of this experimental study is that we were able to grow large, preferentially oriented crystals of olivine and pyroxenes at low cooling rates. These crystals were oriented parallel to the thermal gradient, in the same manner as the megacrysts in natural spinifex-textured komatiites. At cooling rates like those that produce equant, solid crystals in traditional dynamic crystallization experiments, we grew elongate crystals with dendritic morphologies like those of spinifex-textured lavas. The key difference between our experiments and those in earlier studies was the presence of the thermal gradient. We are, therefore, confident that both in the experimental case and in natural komatiite lavas, the presence of this gradient is a key element in the formation of spinifex texture.

Preferred orientation of megacrysts in spinifex-textured lavas

In the experimental charges, as in natural lavas, spinifex-textured olivines or pyroxenes tend to be oriented perpendicular to the cooling front (Fig. 4a and b). This geometry arises because only vertically oriented crystals can grow downward into nutrient-rich liquid, as with Bridgman growth of large single crystals. The others eventually collide with vertical crystals. The preferred

Table 4: Experimental conditions and results of experiments performed with compositions that have clinopyroxene at liquidus

Run	Cooling rate(°C/h)	Thermal gradient(°C/cm)	Starting temperature*	Charge length(cm)	Total run duration(h)	Clinopyroxene in (°C)	Degree of undercooling(°C)	Anorthite in(°C)
Cpx I-1	5	31·9	1211	4·7	23·4	>1233		1160
Cpx I-2	2	30·1	1239	4·0	25·5	1270	35	<1184
Cpx I-9	5	27·4	1356	4·0	27			
Cpx I-10	5	34·4	1287	4·2	42	>1210		1170

*At the top of the charge.

orientation, therefore, results directly from the thermal gradient. Shore & Fowler (1999) have shown that heat is transferred rapidly by radiation along the *a*-axis of elongate olivine crystals. The geometry of the crystal front therefore allows efficient evacuation of latent heat of crystallization from the site of crystallization to the cool end of the capsule, thereby enhancing the thermal gradient effect.

Dendritic morphology

The sketches displaying the positions of crystallization fronts at the time of quenching (Figs 9–11) show a large temperature difference between the equilibrium liquidus and the onset of the olivine crystallization ($-\Delta T$ = 37–56°C, depending on the starting composition). Such a large degree of undercooling is surprising because: (1) Donaldson's (1979) experiments on magnesian silicate liquids showed that, unlike pyroxene and plagioclase, olivine nucleates at minimal degrees of undercooling when the cooling rate is low; (2) in our experiments, olivine grows downward from earlier-formed crystals and nucleation of new crystals is not required. However, Faure *et al.* (2003*a*) found that in conventional dynamic crystallization experiments conducted at high cooling rates (~400°C/h), a large $-\Delta T$ of 60–70°C was also required for the growth of dendritic olivine crystals. The similar degree of undercooling measured in our thermal-gradient experiments and in conventional dynamic crystallization experiments suggests that a large $-\Delta T$ is also responsible for the dendrite morphologies. How does this happen?

The microprobe profiles of glass immediately adjacent to the olivine crystals reveal a boundary layer depleted in the olivine component. This change in chemical composition ahead of the crystal interface affects the liquidus temperature, causing it to decrease around the spinifex tip and to form a zone of constitutional undercooling. The presence of this boundary layer means that the growth of the olivine crystals will be controlled by diffusion (Kirkpatrick, 1981; Baronnet, 1984). Just as during rapid crystallization of strongly oversaturated liquids, the zone of olivine-depleted, constitutionally undersaturated liquid hinders crystal growth and leads to the dendritic morphology (Faure, 2001). We suggest, therefore, that the large $-\Delta T$ is related to the crystal growth process itself, or more specifically, to the rate at which the olivine components diffuse to the crystal and are transferred from liquid to solid. The same conclusion applies to the large, elongate pyroxene crystals.

Crystallization model of spinifex layers

In our experiments, the thermal gradients ranged from about 2·5 to 34·4°C/cm and cooling rates from 2 to 1428°C/h. These rates are equivalent to those in natural komatiite lava flows. In Fig. 19 we show the relation between the two parameters in a relatively thin (2 m) komatiite flow that crystallized from liquid with about 28% MgO, like those described at Pyke Hill (Pyke *et al.*, 1973). Nisbet (1982) and Nisbet *et al.* (1993) estimated the eruption temperature of such a komatiite liquid at about 1560°C. The cooling rates and the variation of thermal gradients with time and depth in the flow can be solved analytically (Jaeger, 1968; Huppert *et al.*, 1984). The temperature of the upper surface is fixed at 0°C and cooling at the lower contact is neglected. By analogy with our experiments with Fo III and Fo VI compositions, a degree of undercooling of komatiite lava equal to 50°C is necessary to obtain crystallization of olivine with dendritic morphology. It is then possible to calculate the cooling rate and the thermal gradient within the flow at the time when olivine crystals developed their dendritic shape and preferential orientation.

Figure 19 shows that when the thickness of the solid to partially crystallized upper margin of the flow has reached 70–80 cm, the cooling rate is less than 10°C/h and the thermal gradient is about 20°C/cm. This depth coincides with the top of the A_3 zone in 2 m thick komatiite flows of Pyke Hill (Pyke *et al.*, 1973). In other words, the conditions under which we produced long dendritic olivine crystals with preferred orientations in our experiments correspond to those during the cooling of komatiite flows with similar textures.

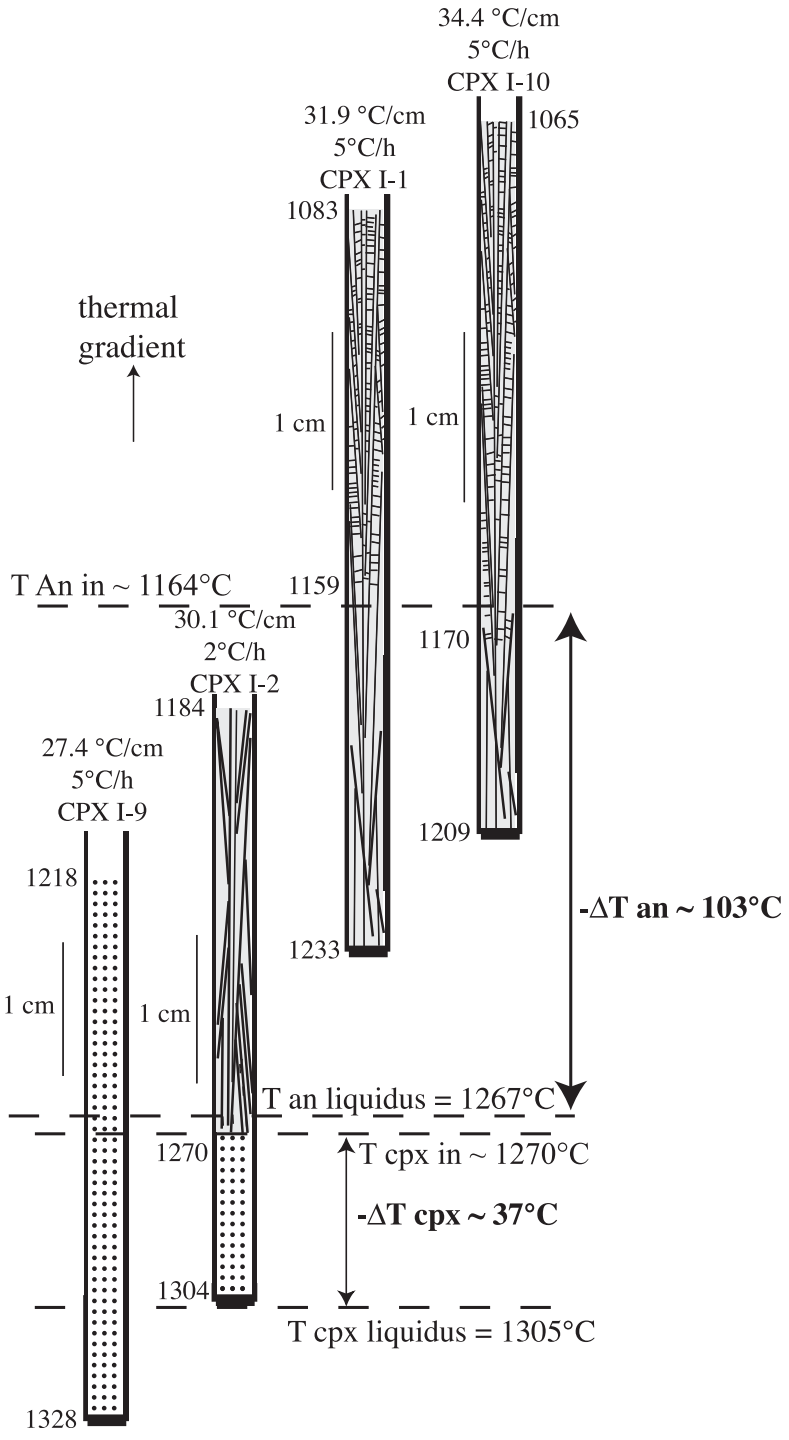

Fig. 16. Sketches displaying the positions of crystallization fronts at the time of quenching in experiments performed with CPX I starting composition. Charge CPX I-9 was totally vitreous although the temperature even at the cold end of the capsule was well below the temperature of the onset of olivine and clinopyroxene crystallization under equilibrium conditions.

More generally, as shown in Fig. 19, the range of conditions in our experiments covers the evolution of conditions from the initial fast cooling in the outer crust of the flow, through cooling at moderate rates in the presence of large thermal gradients in the interior of the spinifex zone, to slower cooling in the presence of a weak thermal gradient in the deep interior of the flow. The chilled margins of komatiite flows normally contain a

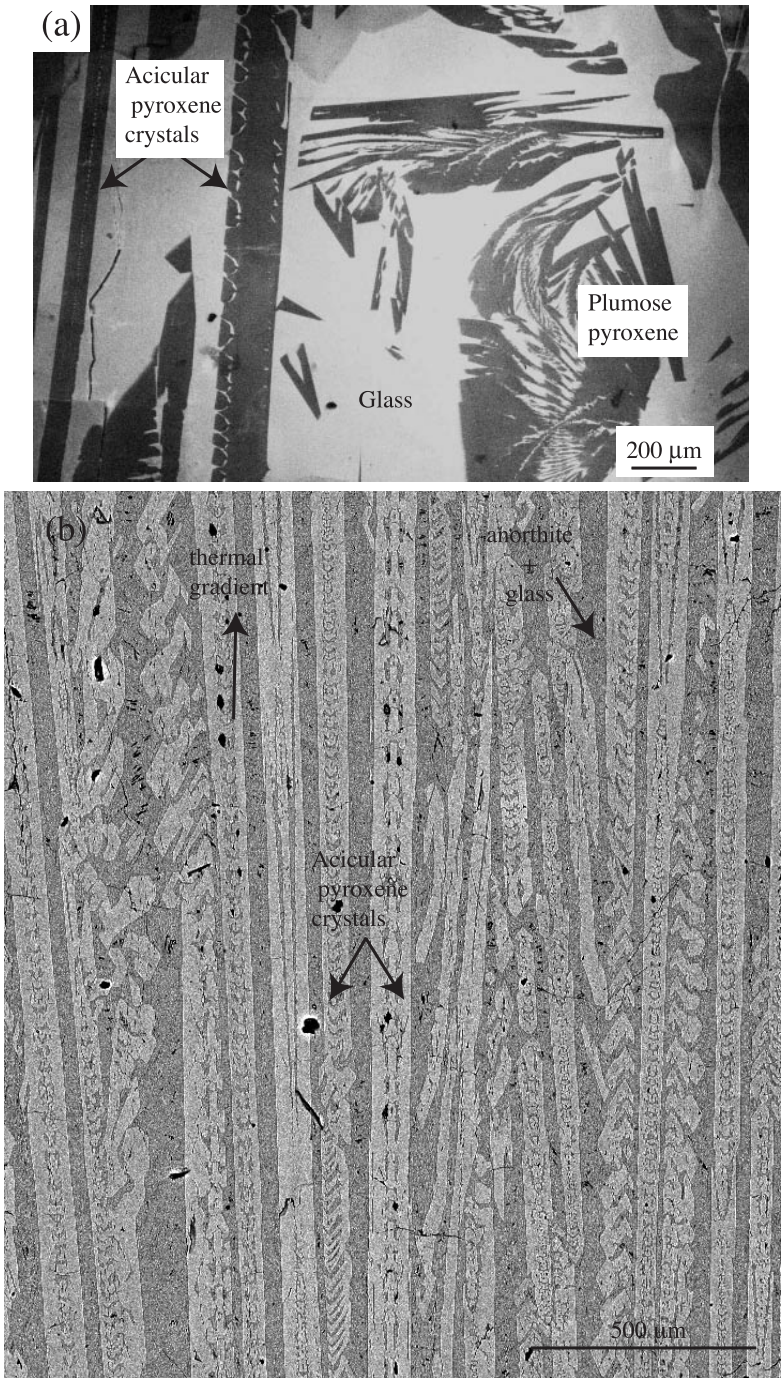

Fig. 17. SEM images showing clinopyroxene morphologies. (a) Cathodoluminescent image of acicular pyroxene crystals oriented parallel to the thermal gradient, and plumose pyroxene set randomly in a glassy matrix (Cpx I-1: cooling rate 5°C/h, thermal gradient 31·9°C/cm). (b) Backscattered electron image of oriented, acicular, spinifex-like pyroxene crystals. The darker area between the acicular crystals is composed of glass and crystals of anorthite. This texture closely resembles 'string-beef' pyroxene spinifex texture in natural komatiitic basalt lavas. (Cpx I-10: cooling rate 5°C/h, thermal gradient 34·4°C/cm).

small fraction (<5 to 20%) of polyhedral olivine phenocrysts, and on this basis it is generally accepted that these lavas erupted at temperatures close to their liquidus (Renner *et al.*, 1994). Although the parental magma may have become superheated as it rose from its deep mantle source along a gradient steeper than the liquidus, the magma must have lost heat and started to crystallize during its passage through the crust and out

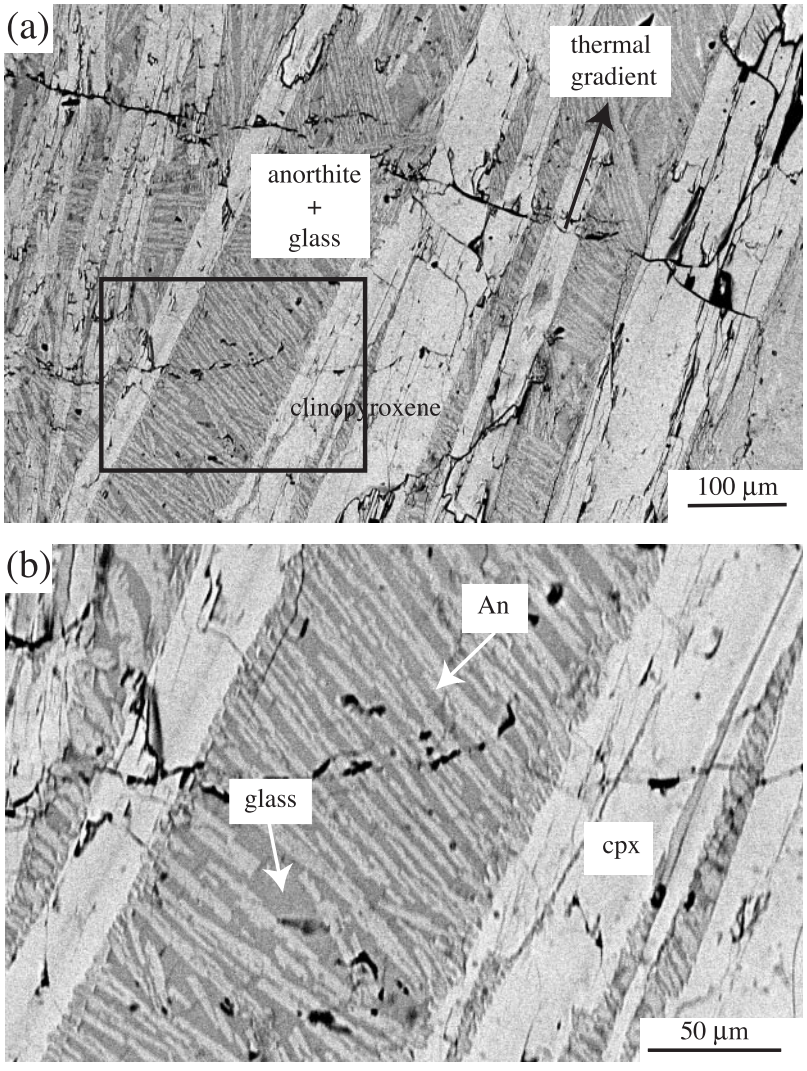

Fig. 18. Backscattered electron images of (a) acicular, spinifex-like pyroxene crystals in a matrix of anorthite and residual glass (Cpx I-1: cooling rate 5°C/h, thermal gradient 31·9°C/cm); (b) enlargement of the area outlined in (a). Anorthite crystals display a preferred orientation and seem to be growing on the acicular clinopyroxene grains.

onto the surface. These olivine grains grew under moderate cooling rates in the absence of a thermal gradient and they have an equant, polyhedral habit. Crystals with this morphology settled to the base of the flow or grew in place to form the lower cumulate zone (Fig. 1).

The initial rapid cooling caused the rapid crystallization that created the random spinifex texture in the upper part of the flow. Conventional dynamic crystallization experiments reproduce these skeletal and dendritic crystals (Donaldson, 1976; Faure *et al.*, 2003*a*) and there is no ambiguity in relating random spinifex to fast cooling rates. Indeed, we demonstrated with our experiments that the thermal gradient has little influence on the crystal habit when the cooling rate is high. Deeper in the lava interior the cooling rate diminishes radically (Donaldson, 1982) and the thermal gradient controls both the morphology of crystals and the preferred orientation of spinifex crystals.

Spinifex layers, therefore, record a two-stage crystallization process. The uppermost layers (A_1 and A_2), where the olivine crystals are small and randomly oriented, correspond to crystallization controlled mainly by cooling rate, whereas the third layer (A_3), where the crystals are larger and oriented perpendicular to the form contact, formed by crystallization controlled by the thermal gradient.

The peculiar morphologies of the chain-like and plumose pyroxene crystals between olivine spinifex crystals in the A_2 and A_3 horizons were interpreted by Fowler *et al.* (2002) as the result of pronounced undercooling or late devitrification of interstitial glass.

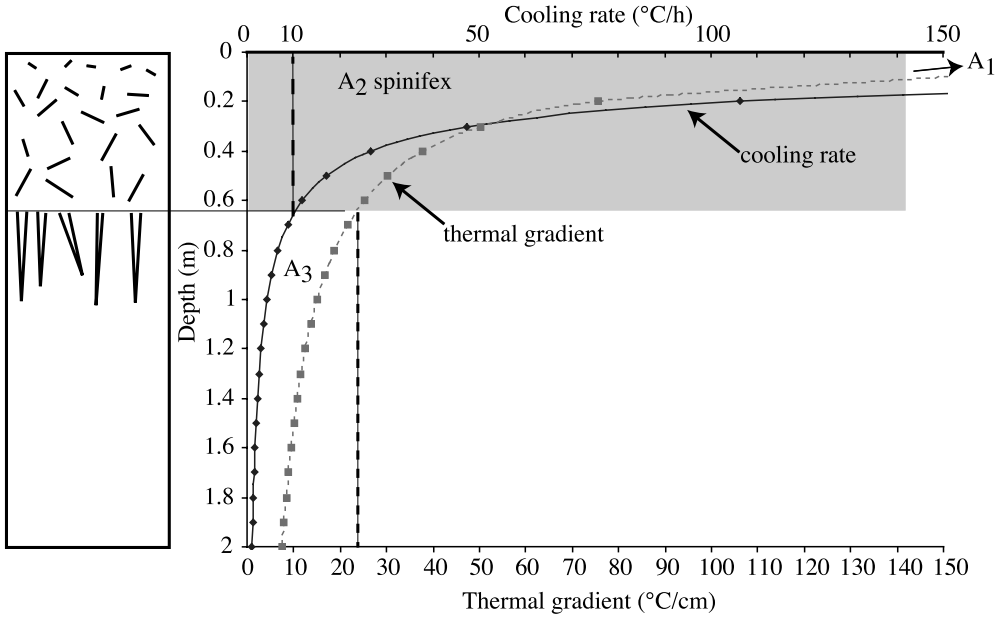

Fig. 19. Diagram illustrating changes in cooling rate and thermal gradient during the crystallization of the upper part of a komatiite flow. In the calculation there was 50°C of undercooling at the time of crystallization. The komatiite liquid was assumed to contain 28% MgO and to have an equilibrium liquidus of 1560°C; the thermal diffusivity used was $9{\cdot}65 \times 10^{-7}$ m^2/s (Renner, 1989). The vertical axis corresponds to depth within the komatiite flow (in m). The A_2 horizon (random spinifex) forms where the cooling rate is >10°C/h. For lower cooling rates, the thermal gradient controlled the morphology and orientation of the olivine crystals, and platy spinifex of the A_3 horizon results. The thermal gradient at this transition is about 20–25°C/cm, a value similar to that used in our experiments. This cooling rate transition is represented in the diagram by the vertical long-dashed line. The corresponding thermal gradient is shown by the vertical short-dashed line.

However, the same type of crystals are present directly above the crystallization front in experimental charges that were quenched from temperatures above the glass transition. These crystals clearly grew from silicate liquid. Their random orientation and location between downward-directed olivine grains suggests further that they grew in the absence of a pronounced thermal gradient. Their chain-like and plumose morphology probably is acquired at the high degree of undercooling brought about by the delay in pyroxene nucleation.

CONCLUSIONS

Our experiments demonstrate that spinifex is a natural consequence of crystallization in the thermal gradient of the crust of a hot, dry komatiite lava flow. In the presence of a temperature gradient, if the cooling rate if not too high (<10°C/h), olivine crystallizes in the form of spinifex blades that form parts of large dendritic crystals and are oriented perpendicular to the cooling front. The effect is most pronounced at low cooling rates of 2–5°C/h, like those estimated during solidification of the central parts of spinifex layers in magnesium-rich lava flows. We have, therefore, found a solution to the paradox surrounding the growth of olivine with dendritic morphology deep in the interior of komatiite lava flows. The dendritic morphology arises from the peculiar geometry associated with constrained crystal growth in the crust of the flow, and is not a consequence of rapid cooling. The presence of water is not a requirement for spinifex texture to form.

Another important result is the measurement of large degrees of undercooling at the onset of the crystallization of olivine and pyroxene in the komatiite experimental charges. For olivine, the degree of undercooling varied between 37 and 56°C, for clinopyroxene the range was from 46 to 56°C. Our experimental configuration affords a unique capacity to measure accurately the degree of undercooling as a function of cooling rate, thermal gradient and starting composition.

ACKNOWLEDGEMENTS

A. Rouillier is thanked for assistance in the high-temperature experimental laboratory of the CRPG-CNRS. We also thank F. Diot for assistance with electron microprobe analyses and SEM at the Service d'Analyses of the Université Henri Poincaré, Nancy. We thank Mike Cheadle, Albert Jambon, Tony Fowler and Claude Herzberg for helpful comments on an early version of the manuscript. This work was supported by INSU through a PNP grant (to G.L and N.A.).

REFERENCES

Aitken, B. G. & Echeverria, L. M. (1984). Petrology and geochemistry of komatiites and tholeiites from Gorgona Island, Colombia. *Contributions to Mineralogy and Petrology* **86**, 94–105.

Arndt, N. T. (1976). Melting relations of ultramafic lavas (komatiites) at 1 atm and high pressure. *Carnegie Institution of Washington Yearbook* **75**, 555–562.

Arndt, N. T. (1994). Archean komatiites. In: Condie, K. C. (ed.) *Archean Crustal Evolution*. Amsterdam: Elsevier, pp. 11–44.

Arndt, N. T. (2003). Komatiites, kimberlites and boninites. *Journal of Geophysical Research* **108** (ECV5), 1–11.

Arndt, N. T. & Fleet, M. E. (1979). Stable and metastable pyroxene crystallization in layered komatiite flows. *American Mineralogist* **64**, 856–864.

Arndt, N. T., Naldrett, A. J. & Pyke, D. R. (1977). Komatiitic and iron-rich tholeiitic lavas of Munro Township, northeast Ontario. *Journal of Petrology* **18**, 319–369.

Arndt, N., Ginibre, C., Chauvel, C., Albarède, F., Cheadle, M., Herzberg, C., Jenner, G. & Lahaye, Y. (1998). Were komatiites wet? *Geology* **26**, 739–742.

Baronnet, A. (1984). Growth kinetics of the silicates. A review of basic concepts. *Fortschritte der Mineralogie* **62**, 187–232.

Dann, J. C. (2000). The Komati Formation, Barberton Greenstone Belt, South Africa, part I: new map and magmatic architecture. *South African Journal of Geology* **103**, 47–68.

Dann, J. C. (2001). Vesicular komatiites, 3·5-Ga Komati Formation, Barberton Greenstone Belt, South Africa: inflation of submarine lavas and origin of spinifex zones. *Bulletin of Volcanology* **63**, 462–481.

Donaldson, C. H. (1976). An experimental investigation of olivine morphology. *Contributions to Mineralogy and Petrology* **57**, 187–213.

Donaldson, C. H. (1979). An experimental investigation of the delay in nucleation of olivine in mafic magmas. *Contributions to Mineralogy and Petrology* **69**, 21–32.

Donaldson, C. H. (1982). Spinifex-textured komatiites: a review of textures, compositions and layering. In: Arndt, N. T. & Nisbet, E. G. (eds) *Komatiites*. London: Allen & Unwin, pp. 213–244.

Faure, F. (2001). Les textures de croissance rapide dans les roches magmatiques basiques et ultrabasiques: étude expérimentale et nanoscopique. Ph.D. thesis, Clermont-Ferrand University, 252 pp.

Faure, F. & Schiano, P. (2004). Crystal morphologies in pillow basalts: implications for mid-ocean ridge processes. *Earth and Planetary Science Letters* **220**, 331–344.

Faure, F. & Schiano, P. (2005). Experimental investigation of equilibration conditions during forsterite growth and melt inclusion formation. *Earth and Planetary Science Letters* **236**, 882–898.

Faure, F., Trolliard, G., Nicollet, C. & Montel, J. M. (2003*a*). A developmental model of olivine morphology as a function of the cooling rate and the degree of undercooling. *Contributions to Mineralogy and Petrology* **145**, 251–263.

Faure, F., Trolliard, G. & Soulestin, B. (2003*b*). TEM investigation of forsterite dendrites. *American Mineralogist* **88**, 1241–1250.

Fleet, M. E. & McRae, N. D. (1975). A spinifex rock from Munro Township, Ontario. *Canadian Journal of Earth Sciences* **12**, 928–939.

Fowler, A. D., Berger, B., Shore, M., Jones, M. I. & Ropchan, J. (2002). Supercooled rocks: development and significance of varioles, spherulites, dendrites and spinifex in Archaean volcanic rocks, Abitibi Greenstone Belt, Canada. *Precambrian Research* **115**, 311–328.

Ginibre, C., Arndt, N. T., Hallot, E., Lesher, C. M. & Cashman, K. V. (1997). An experimental study of spinifex textures in komatiites from Gorgona, Colombia. *Terra Nova* **9**, 203.

Grove, T. L. (1978). Cooling histories of Luna 24 very low (VLT) ferrobasalts: an experimental study. *Proceeding of the 9th Lunar and Planetary Science Conference. Geochimica et Cosmochimica Acta Supplement* **9**, 565–584.

Grove, T. L., Gaetani, G. A. & deWit, M. J. (1994). Spinifex textures in 3·49 Ga Barberton Mountain Belt komatiites: evidence for crystallization of water-bearing, cool magmas in the Archean. *EOS Transactions, American Geophysical Union* **75**, 354.

Grove, T. L., Gaetani, G. A., Parman, S., Dann, J. & deWit, M. J. (1996). Origin of spinifex textures in 3·46 Ga komatiite magmas from the Barberton Mountainland, South Africa. *EOS Transactions, American Geophysical Union* **77**, 281.

Grove, T. L., Parman, S. W., Nuka, P., DeWit, M. & Dann, J. (2002). Influence of H_2O on the development of spinifex textures in komatiites. *Geochimica et Cosmochimica Acta* **66**, 294.

Huppert, H. E., Sparks, R. J. S., Turner, J. S. & Arndt, N. T. (1984). The emplacement and cooling of komatiite lavas. *Nature* **309**, 19–23.

Jaeger, J. C. (1968). Cooling and solidification of igneous rocks. In: Hess, H. H. & Poldervaart,A. (eds) *Basalts: the Poldervaart Treastise on Rocks of Basaltic Composition*. New York: John Wiley–Interscience.

Jerram, D. A., Cheadle, M. J. & Philpotts, A. R. (2003). Quantifying the building blocks of igneous rocks: are clustered crystal frameworks the foundation? *Journal of Petrology* **44**, 2033–2051.

Kirkpatrick, R. J. (1978). Processes of crystallization in pillow basalts, hole 396B, DSDP LEG 46. In: Dmitriev, L., Heirtzler, J. *et al.* (eds) *Initial Reports of the Deep Sea Drilling Project, 46*. Washington, DC: US Government Printing Office, pp. 271–280.

Kirkpatrick, R. J. (1981). Kinetics of crystallization of igneous rocks. In: Lasaga, A. C. & Kirkpatrick, R. J. (eds) *Kinetics of Geochemical Processes. Mineralogical Society of America, Reviews in Mineralogy* **8**, 321–398.

Kirkpatrick, R. J., Robinson, G. R. & Hays, J. F. (1976). Kinetics of crystal growth from silicate melts: anorthite and diopside. *Journal of Geophysical Research* **81**, 5715–5720.

Kirkpatrick, R. J., Kuo, L. C. & Melchior, J. (1981). Crystal growth in incongruently-melting compositions: programmed cooling experiments with diopside. *American Mineralogist* **66**, 223–241.

Latypov, R. M. (2003). The origin of marginal compositional reversals in basic–ultrabasic sills and layered intrusions by Soret fractionation. *Journal of Petrology* **44**,1579–1618.

Lesher, C. E., Cashman, K. V. & Mayfield, J. D. (1999). Kinetic controls on crystallization of Tertiary North Atlantic basalt and implications for the emplacement and cooling history of lava at site 989, southeast Greenland rifted margin. In: Larsen, H. C., Duncan, R. A., Allan, J. F. & Brooks, K. (eds) *Proceedings of the Ocean Drilling Program, Scientific Results, 163*. College Station, TX: Ocean Drilling Program, pp. 135–148.

Lofgren, G. (1989). Dynamic crystallization of chondrule melts of porphyritic olivine composition: textures experimental and natural. *Geochimica et Cosmochimica Acta* **53**, 461–470.

Nesbitt, R. W. (1971). Skeletal crystal forms in the ultramafic rocks of the Yilgarn Block, Western Australia: evidence for an Archaean ultramafic liquid. *Geological Society of Australia* **3**, 331–347.

Nisbet, E. G. (1982). The tectonic setting and petrogenesis of komatiites. In: Arndt, N. T. & Nisbet, E. G. (eds) *Komatiites*. London: Allen & Unwin, pp. 501–520.

Nisbet, E. G., Cheadle, M. J., Arndt, N. T. & Bickle, M. J. (1993). Constraining the potential temperature of the Archaean mantle: a review of the evidence from komatiites. *Lithos* **30**, 296–307.

Parman, S. W., Dann, J. C., Grove, T. L. & deWit, M. J. (1997). Emplacement conditions of komatiite magmas from the 3·49 Ga Komati Formation, Barberton Greenstone Belt, South Africa. *Earth and Planetary Science Letters* **150**, 303–323.

Pyke, D. R., Naldrett, A. J. & Eckstrand, O. R. (1973). Archean ultramafic flows in Munro Township. *Geological Society of American Bulletin* **4**, 955–978.

Renner, R. (1989). Cooling and crystallization of komatiite flows from Zimbabwe. Ph.D. thesis, Cambridge University, 162 pp.

Renner, R., Nisbet, E. G., Cheadle, M. J., Arndt, N. T., Bickle, M. J. & Cameron, W. E. (1994). Komatiite flows from the Reliance formation, Belingwe Belt, Zimbabwe: 1. Petrography and mineralogy. *Journal of Petrology* **35**, 361–400.

Roeder, P. L., Poustovetov, A. & Oskarsson, N. (2001). Growth forms and composition of chromian spinel in MORB magma: diffusion-controlled crystallization of chromian spinel. *Canadian Mineralogist* **39**, 397–416.

Roeder, P. L., Thornber, C., Poustovetov, A. & Grant, A. (2003). Morphology and composition of spinel in Pu'u 'O'o lava (1996–1998), Kilauea volcano, Hawaii. *Journal of Volcanology and Geothermal Research* **123**, 245–265.

Schwindinger, K. R. & Anderson, J. A. T. (1989). Synneusis of Kilauea Iki olivines. *Contributions to Mineralogy and Petrology* **103**, 187–198.

Shore, M. & Fowler, A. D. (1999). The origin of spinifex texture in komatiites. *Nature* **397**, 691–694.

Turner, S., Huppert, H. E. & Sparks, R. S. J. (1986). Komatiites II: experimental and theoretical investigations of post-emplacement cooling and crystallization. *Journal of Petrology* **27**, 397–437.